Generalised Pre-coding Aided Spatial Modulation

Rong Zhang, Lie-Liang Yang and Lajos Hanzo

***Abstract*—A new Multiple Input Multiple Output (MIMO) transmission scheme termed as Generalised Pre-coding aided Spatial Modulation (GPSM) is proposed, where the key idea is that a particular subset of *receive* antennas is activated and the activation pattern itself conveys useful information. This is in contrast to the previously proposed Spatial Modulation (SM) schemes, which operated by activating a specific subset of *transmit* antennas. We provide both analytical and numerical results characterizing the GPSM scheme proposed for both conventional as well as for large-dimensional MIMO configurations subject to both realistic imperfect Channel State Information at the Transmitter (CSIT) and to the low-rank approximation invoked for large-dimensional MIMO configurations. We also design a so-called reinforcement matrix for attaining substantial performance improvements for our proposed GPSM scheme. Our investigations show that the GPSM scheme constitutes a flexible alternative to the state-of-the-art MIMO transmission schemes, especially because it is capable of achieving a high throughput. Moreover, the benefits of mapping information to the spatial domain rather than relying on conventional modulation has substantial benefits in the medium to high Signal to Noise Ratio (SNR) region. Quantitatively, GPSM is capable of supporting the same throughput as the conventional full-multiplexing gain based MIMO arrangements at an SNR gain of about 1dB at the same receiver complexity. Furthermore, the reinforcement matrix aided GPSM scheme attains a further 3-4dB performance improvement as compared to the conventional GPSM scheme.**

***Index Terms*—**

I. INTRODUCTION

MULTIPLE Input Multiple Output (MIMO) systems constitute one of the most promising technical advances in wireless communications [1], since they facilitate high-throughput transmissions in the context of various standards [2]. Hence, they attracted substantial research interests, leading to the Vertical-Bell Laboratories Layered Space-Time (V-BLAST) [3] and Space Time Block Coding (STBC) [4] etc. The point-to-point single-user MIMO systems are capable of offering diverse transmission functionalities in terms of multiplexing, diversity and beam-forming gains, while in a multi-user MIMO context, Space Division Multiple Access (SDMA) employed in the uplink and downlink constitute beneficial building blocks [5]. The basic benefits of MIMOs have also been further exploited in the context of the Network MIMO [6], massive MIMO [7] and interference-limited MIMO [8] concepts.

Despite having a plethora of studies on classic MIMO systems, their practical constraints, such as their I/Q imbalance, their transmitter and receiver complexity as well as the cost of their multiple Radio Frequency (RF) Power Amplifiers (PA), Digital-Analogue / Analogue-Digital (DA/AD) converters etc have received limited attention [9], despite the many-fold benefits of MIMO systems. To circumvent these problems, low complexity alternatives to conventional MIMO transmission schemes have also been proposed, such as the Antenna Selection (AS) [10] and the Spatial Modulation (SM) [11] philosophies, where AS constitutes an attractive use of MIMOs associated with a low front-end complexity, which is achieved by switching a subset of all available antenna elements in both/either the transmitter and/or receiver. This scheme benefits from a high diversity gain and it is also robust to channel estimation errors. Hence it has been adopted in the Long Term Evolution (LTE) system's uplink. On the other hand, SM constitutes a novel MIMO technique, which is motivated by the goal of providing a higher throughput than a single-antenna aided system, while maintaining both a lower complexity and a lower cost than the conventional MIMOs. Since only one transmit antenna is activated at a time, traditional problems associated with MIMOs, such as the Inter-Channel-Interference (ICI) and Inter-Antenna-Synchronisation (IAS) are avoided.

To elaborate a little further, SM conveys extra information by mapping additional bits to the *transmit* antenna indices in addition to the classic modulation schemes as detailed in [12], [13]. The detailed analysis of SM has been conducted under different channel statistics [14], its selection criterion has been designed in [15] and a diverse range of beneficial extensions, such as trellis coded SM [16] and STBC based SM [17] have also been proposed in the literature. More explicitly, for trellis coded SM, the transmit antennas are partitioned into subsets and the resultant spatial spacing between the antennas within each subset is maximized for the sake of mitigating the undesirable channel correlation. On the other hand, STBC based SM exploits the space-, time- and antenna-domain for conveying information. The resultant hybrid system benefits from the diversity gain of the STBC scheme. The meritorious implementation of SM in the context of Space Shift Keying (SSK) [18], [19] and its higher-throughput version termed as generalised SM [20], [21] constitute further important relatives. On the other hand, the Pre-coding aided Spatial Modulation (PSM) schemes conveying extra information by appropriately selecting the *receive* antenna indices were investigated in [22] and also discussed in [23]. More explicitly, in PSM the indices of the receive antennas represent additional

Manuscript received DATE; revised DATE; accepted DATE. The associate editor coordinating the review of this paper and approving it for publication was NAME.

The authors are with the Communications, Signal Processing and Control, School of ECS, University of Southampton, SO17 1BJ, UK (e-mail: {rz, lly, lh}@ecs.soton.ac.uk).

The financial support of the EPSRC under the India-UK Advanced Technology Centre (IU-ATC), that of the EU under the concerto project as well as that of the European Research Council's (ERC) Advanced Fellow Grant is gratefully acknowledged.

Digital Object Identifier 10.1109/TWC.2013.130848.

information in the spatial domain. As a specific counterpart of the original SM, PSM benefits from both a low cost and complexity at the receiver side, therefore it may be considered to be most suitable for downlink transmission.

Hence, in this paper, we extend and generalise the PSM scheme of [22] to offer a full treatment, where *we propose the Generalised Pre-coding Aided Spatial Modulation (GPSM) concept as a new MIMO transmission scheme. We commence by its analytical study under the idealised simplifying assumption of having perfect Channel State Information at the Transmitter (CSIT). Then two practical issues are investigated, namely the detrimental impact of realistic imperfect CSIT followed by a low-rank approximation invoked for large-dimensional MIMOs. Furthermore, we propose a reinforcement matrix aided GPSM scheme, which is capable of boosting the performance of GPSM.*

The rest of our paper is organised as follows. In Section II, we introduce the concept as well as the detection methods of the GPSM scheme under the idealised simplifying assumption of having perfect CSIT, which is complemented by our discussions on the associated detection complexity. This is followed by our analytical study in Section III under the perfect CSIT assumption as well as by our investigations of the impact of realistic imperfect CSIT, of a low-rank approximation and of a reinforcement matrix aided enhancement. Our simulation results are provided in Section IV, while we conclude in Section V.

Notations: In this paper, we use lower-case bold variable to represent a vector and capital bold fonts to represent a matrix. The operator $\mathbb{E}$ represents expectation, Tr denotes the trace of a square matrix, $\mathcal{R}$ represents taking the real part and $\lfloor . \rfloor$ indicates flooring operator. In addition, the superscripts $()^T$ and $()^*$ represent matrix transpose and matrix conjugate, respectively, while we use $()^H$ to represent the matrix transpose and conjugate.

II. System Description

Consider a MIMO system equipped with N_t transmit antennas and N_r receive antennas, where we assume $N_t \geq N_r$. In this MIMO set-up, a maximum of $N_s = \min(N_t, N_r) = N_r$ parallel data streams may be supported, conveying a total of $k_{eff} = N_r k_{mod}$ bits altogether, where $k_{mod} = \log_2(M)$ denotes the number of bits per symbol of a conventional M-ary PSK/QAM scheme [13], [24]. Transmitter pre-coding relying on the matrix $\boldsymbol{P} \in \mathbb{C}^{N_t \times N_r}$ may be used for proactively mitigating the ICI at the transmitter by preprocessing the source signal before its transmission by exploiting the CSIT [25]. As a benefit, a low-complexity single-stream detection scheme may be used by the downlink receiver, because the ICI is eliminated at the downlink transmitter.

A. Pre-coding Aided Spatial Modulation

1) Concept: In contrast to the above-mentioned classic full-multiplexing of N_r data streams, the concept of PSM relies on activating one out of N_r receive antennas with the aid of transmitter pre-coding, where the particular choice of the receive antenna activated conveys extra information in addition to the information carried by the conventional modulated symbols mapped to it. More explicitly, in the PSM arrangement, only the kth receive antenna is activated by the spatial symbol $k \in \mathcal{Z}$, where $\mathcal{Z} = \{1, \ldots, N_r\}$ denotes the indices of activated receive antennas.

More explicitly, the spatial modulated *super-symbol* $\boldsymbol{s} \in \mathbb{C}^{N_r \times 1}$ is constituted by an all-zero vector, except for its kth entry occupied by the conventional modulated symbol $b_m \in \mathcal{A}$ and $\mathbb{E}[|b_m|^2] = 1$, where $\mathcal{A}$ denotes the alphabet of a particular M-ary PSK/QAM scheme. Let $\boldsymbol{s}_m^k$ be an *explicit* representation of the super-symbol $\boldsymbol{s}$, indicating the transmission of b_m by activating the kth antenna. Mathematically, it can be written as $\boldsymbol{s}_m^k = \boldsymbol{e}_k b_m$, where $\boldsymbol{e}_k$ is the kth column of an identity matrix of size N_r, representing its activation by the spatial symbol k. As a result, the total number of bits transmitted by the PSM scheme is $k_{eff} = k_{ssk} + k_{mod}$, where $k_{ssk} = \log_2(N_r)$ is the extra information conveyed by the spatial symbol.

After transmitter pre-coding, the resultant transmit signal $\boldsymbol{x} \in \mathbb{C}^{N_t \times 1}$ can be written as

$$\boldsymbol{x} = \boldsymbol{P}\boldsymbol{s}_m^k. \tag{1}$$

In order to avoid power amplification during the pre-processing, i.e. for the sake of maintaining $\mathbb{E}[||\boldsymbol{x}||^2] = 1$, we have to impose the constraint $\mathrm{Tr}\{\boldsymbol{P}\boldsymbol{P}^H\} = N_r$ on the pre-coding matrix.

2) Design: The signal observed at the N_r receive antennas may be written as

$$\boldsymbol{y} = \boldsymbol{H}^T \boldsymbol{P}\boldsymbol{s}_m^k + \boldsymbol{w}, \tag{2}$$

where $\boldsymbol{w} \in \mathbb{C}^{N_r \times 1}$ is the circularly symmetric complex Gaussian noise vector with each entry having a zero mean and a variance per dimension of $\sigma^2 = N_0/2$, i.e. $w_j \sim \mathcal{CN}(0, N_0), \forall j$, while $\boldsymbol{H} \in \mathbb{C}^{N_t \times N_r}$ represents the MIMO channel involved. We assume furthermore that each entry of $\boldsymbol{H}$ undergoes frequency-flat Rayleigh fading and it is uncorrelated between different super-symbol transmissions, while remains static within the duration of a super-symbol's transmission. The super-symbols transmitted are statistically independent from the noise.

Hence, the pre-coding matrix designed would have to maximize the desired decision D_0 associated with super-symbol $\boldsymbol{s}_m^k$ and simultaneously minimize the undesired i.e. erroneous decisions D_1 associated with all other super-symbols $\boldsymbol{s}_n^j, \forall j \neq k, \forall n \neq m$. Mathematically, the optimum pre-coding matrix $\boldsymbol{P}^o$ should satisfy

$$\boldsymbol{P}^o = \arg\max_{\boldsymbol{P}} \{D_0 - D_1\}, \tag{3}$$

where the desired decision D_0 may be written as

$$\begin{aligned} D_0 &= -||\boldsymbol{y} - \boldsymbol{s}_m^k||^2 \\ &\propto 2\mathcal{R}\{\boldsymbol{y}^H \boldsymbol{s}_m^k\} - ||\boldsymbol{s}_m^k||^2 \\ &\propto 2\mathcal{R}\{(\boldsymbol{s}_m^k)^H \boldsymbol{P}^H \boldsymbol{H}^* \boldsymbol{s}_m^k + \boldsymbol{w}^H \boldsymbol{s}_m^k\} - ||\boldsymbol{s}_m^k||^2, \end{aligned} \tag{4}$$

while the undesired decisions D_1 may be written as

$$\begin{aligned} D_1 &= \sum_{j\neq k}\sum_{n\neq m} -||\boldsymbol{y}-\boldsymbol{s}_n^j||^2 \\ &\propto \sum_{j\neq k}\sum_{n\neq m} 2\mathcal{R}\{\boldsymbol{y}^H\boldsymbol{s}_n^j\} - ||\boldsymbol{s}_n^j||^2 \\ &\propto \sum_{j\neq k}\sum_{n\neq m} 2\mathcal{R}\{(\boldsymbol{s}_n^j)^H\boldsymbol{P}^H\boldsymbol{H}^*\boldsymbol{s}_n^j + \boldsymbol{w}^H\boldsymbol{s}_n^j\} - ||\boldsymbol{s}_n^j||^2. \quad (5) \end{aligned}$$

To achieve the above objective, the pre-coding matrix has to ensure that no energy leaks into the unintended receive antennas. In other words, we capture all the energy by the kth receive antenna. Hence, the so-called Minimum-Power Distortionless Response (MPDR) of [26] design criterion can be employed in form of its typical instantiations, namely the Zero Forcing (ZF) pre-coding and the Minimum Mean Square Error (MMSE) pre-coding. In this paper, we take ZF pre-coding into consideration. More explicitly, the ZF pre-coding [27] constitutes the pseudo-inverse of the MIMO channel $\boldsymbol{H}^T$, which is written as

$$\boldsymbol{P} = \beta\boldsymbol{H}^*(\boldsymbol{H}^T\boldsymbol{H}^*)^{-1}, \quad (6)$$

where $\beta = \sqrt{N_r/\mathrm{Tr}[(\boldsymbol{H}^T\boldsymbol{H}^*)^{-1}]}$ is a normalisation factor. Note that letting simply $\beta = \sqrt{N_t}$ also satisfies our power constraint statistically.

3) Detection: When ZF pre-coding is employed, the received signal can be further written as

$$\boldsymbol{y} = \beta\boldsymbol{s}_m^k + \boldsymbol{w}, \quad (7)$$

which may be decomposed into

$$y_k = \beta b_m + w_k; \qquad y_j = w_j, \qquad \forall j \neq k. \quad (8)$$

Hence the joint detection of both the conventional modulated symbol b_m and of the spatial symbol k obeys the Maximum Likelihood (ML) criterion. More explicitly, we have

$$[\hat{m},\hat{k}] = \arg\min_{\boldsymbol{s}_n^j\in\mathcal{B}}\{||\boldsymbol{y}/\beta - \boldsymbol{s}_n^j||^2\}, \quad (9)$$

where $\mathcal{B} = \mathcal{Z}\times\mathcal{A}$ stands for the super-alphabet of the super-symbol $\boldsymbol{s}_n^j$. Alternatively, decoupled detection may also be employed, which treats the detection of the conventional modulated symbol b_m and the spatial symbol k separately. In this low-complexity variant, we have

$$\hat{k} = \arg\max_{j\in[1,N_r]}\{|y_j|^2\} \quad (10)$$

$$\hat{m} = \arg\max_{n\in[1,M]}\{|y_{\hat{k}}/\beta - b_n|^2\}. \quad (11)$$

Thus, correct detection is declared, when we have $\hat{k}=k$ and $\hat{m}=m$.

B. Generalisation

The main limitation of the above-mentioned standard PSM is that only a single receive antenna is activated at a time, which naturally limits the flexibility of PSM. Hence, we generalise it to allow the activation of multiple receive antennas.

1) Concept: In our GPSM scheme, a total of $N_a < N_r$ receive antennas are activated so as to facilitate the simultaneous transmission of N_a data streams. Hence, the number of bits in GPSM conveyed by a spatial symbol becomes $k_{ssk} = \lfloor\log_2(|\mathcal{C}_t|)\rfloor$, where the set $\mathcal{C}_t$ contains all the combinations associated with choosing N_a active receive antennas from N_r receive antennas. Thus the effective number of bits transmitted by our GPSM scheme is $k_{eff} = k_{ssk} + N_a k_{mod}$.

Unlike in standard PSM, where each spatial symbol corresponds to a particular receive antenna, each spatial symbol in GPSM corresponds to a particular *pattern* of N_a activated receive antennas.

Example II.1. *For example, activating $N_a = 2$ receive antennas from $N_r = 4$ receive antennas results in a total of $|\mathcal{C}_t| = 6$ legitimate activation patterns, i.e. the patterns of $\mathcal{C}_t = \{[1,2],[1,3],[1,4],[2,3],[2,4],[3,4]\}$. This configuration delivers $k_{ssk} = 2$ bits of information because $\lfloor\log_2(|6|)\rfloor = 2$, albeit only $2^{k_{ssk}} = 4$ out of $|\mathcal{C}_t| = 6$ patterns are required for the actual transmission of two bits. Let us define the set of selected activation patterns as $\mathcal{C}\subset\mathcal{C}_t$. Upon selecting for example $\mathcal{C} = \{\mathcal{C}_t(1),\mathcal{C}_t(2),\mathcal{C}_t(3),\mathcal{C}_t(4)\}$, we have the mapping between the spatial symbol and the pattern of activated receive antennas as*

$$\begin{aligned} k=1 &\mapsto \mathcal{C}(1)=[1,2] \qquad & k=2 &\mapsto \mathcal{C}(2)=[1,3] \\ k=3 &\mapsto \mathcal{C}(3)=[1,4] \qquad & k=4 &\mapsto \mathcal{C}(4)=[2,3] \end{aligned}$$

Note that, the above pattern is not a balanced pattern thus the receive antennas are not uniformly activated. In this paper, we simply opt for $\mathcal{C} = \{\mathcal{C}_t(1),\ldots,\mathcal{C}_t(2^{k_{ssk}})\}$, while the optimisation of pattern selection will be left for our future work. Furthermore, we let $\mathcal{C}(k)$ and $\mathcal{C}(k,i)$ denote the kth activation pattern and the ith activated receive antenna in the kth activation pattern, respectively. We also let $\boldsymbol{s}_m^k$ be an *explicit* representation of the super-symbol $\boldsymbol{s}$, indicating that the receive antenna pattern k is activated and N_a conventional modulated data streams $\boldsymbol{b}_m = [b_{m_1},\ldots,b_{m_{N_a}}]$ are transmitted. In other words, we can revise the expression of the spatially modulated super-symbol as $\boldsymbol{s}_m^k = \boldsymbol{\Omega}_k\boldsymbol{b}_m$, where $\boldsymbol{b}_m\in\mathbb{C}^{N_a\times 1}$ contains N_a conventional modulated data streams of our GPSM scheme and $\boldsymbol{\Omega}_k = \boldsymbol{I}[\mathcal{C}(k)]\in\mathbb{B}^{N_r\times N_a}$ is constituted by the selected columns of an identity matrix of size N_r, where the specific selection is denoted by $\mathcal{C}(k)$ and $\mathbb{B}^{N_r\times N_a}$ represents a $(N_r\times N_a)$-element matrix having binary entries.

2) Detection: When ZF pre-coding is employed, the signal observed at the N_r receive antennas may be written as $\boldsymbol{y} = \beta\boldsymbol{s}_m^k + \boldsymbol{w}$. As in the standard PSM, we have two optional detection algorithms. When joint detection is considered, similar to (9), we have

$$[\hat{m}_1,\ldots,\hat{m}_{N_a},\hat{k}] = \arg\min_{\boldsymbol{s}_n^j\in\mathcal{B}}\{||\boldsymbol{y}/\beta - \boldsymbol{s}_n^j||^2\}, \quad (12)$$

where $\mathcal{B} = \mathcal{C}\times\mathcal{A}^{N_a}$ is the joint search space of the super-symbol $\boldsymbol{s}_n^j$. On the other hand, when separate detection is

considered, we have

$$\hat{k} = \arg \max_{j \in [1, |\mathcal{C}|]} \{ \sum_{i=1}^{N_a} |y_{\mathcal{C}(j,i)}|^2 \} \quad (13)$$

$$\hat{m}_i = \arg \max_{n_i \in [1,M]} \{ |y_{\mathcal{C}(\hat{k},i)}/\beta - b_{n_i}|^2 \}, \quad (14)$$

where (14) has to be evaluated for all N_a data streams and correct detection is declared, when we have $\hat{k} = k$ and $\hat{m}_i = m_i, \forall i$.

It is thus plausible that the standard PSM scheme constitutes a special case of GPSM for $N_a = 1$ and the detection scheme of (13) is non-coherent, while that of (14) only requires the knowledge of the scaling factor β.

3) Complexity: Let us now discuss the complexity of the GPSM scheme in comparison to the conventional pre-coding aided MIMO arrangement supporting N_r data streams. We first note that the transmitter pre-coding exhibits the same complexity in both schemes, hence our focus is on the detection complexity at the receiver.

In conventional MIMO arrangements, when transmitter pre-coding is capable of perfectly separating the N_r parallel data streams, such as the ZF pre-coding, low-complexity single-stream detection is facilitated at the receiver. Hence, the detection complexity increases linearly with the number of receive antennas N_r, but exponentially with the number of bits per symbol in the M-ary PSK/QAM scheme employed. Hence, we may characterise the complexity order as $\mathcal{O}(N_r M)$.

On the other hand, in the GPSM scheme, the complexity of the joint detection of (12) is quite high, which is on the order determined by the super-alphabet $\mathcal{B}$, i.e. obeys $\mathcal{O}(|\mathcal{C}|M^{N_a})$. By contrast, the separate detection of (13) and (14) facilitates a substantially reduced complexity. More explicitly, the complexity is imposed by detecting N_a data streams as in a conventional MIMO arrangement, plus the complexity (Δ) imposed by the comparisons invoked for detecting the spatial symbol, which may be written as $\mathcal{O}(N_a M + \Delta)$.

To elaborate a little further, in the separate detection regime, the number of multiplications required by (13) is N_r, regardless of the value of N_a, because only N_r antenna waveforms have to be considered in the computations. To evaluate the number of multiplications required by (14), we rewrite it as

$$\begin{aligned} \hat{m}_i &= \arg \max_{n_i \in [1,M]} \{ |y_{\mathcal{C}(\hat{k},i)}/\beta - b_{n_i}|^2 \} \\ &= \arg \min_{n_i \in [1,M]} \{ 2\mathcal{R}\{ y_{\mathcal{C}(\hat{k},i)} b_{n_i}/\beta \} - |b_{n_i}|^2 \}. \end{aligned} \quad (15)$$

Hence the number of multiplications required by (15) is simply $2M$. As a result, the total number of multiplications required for detecting N_a data streams is $(M + N_a M)$ rather than $2N_a M$, because the computation of $|b_{n_i}|^2$ is shared by all N_a computations of (15), when all N_a data streams use the same modulation. Hence, the total number of multiplications required in GPSM using separate detection is $\chi_{GPSM} = N_r + M + N_a M$. By contrast, conventional MIMO arrangements may be viewed as a special case of GPSM, when we have $N_a = N_r$ and dispensing with the computation of (13). Naturally, the total number of multiplications required in conventional MIMO schemes is $\chi_{MIMO} = M + N_r M$.

Remark: We carry out a direct comparison between the GPSM and the conventional pre-coding aided MIMO scheme, since they both require DL pre-processing and CSIT. This constitutes the main difference between our PSM/GPSM and the classic SM/GSM [12], [20], [21], although they may be considered as dual pair of each other. As a result, the comparisons between PSM/GPSM and SM/GSM cannot be readily made under identical circumstances, because

- the inevitable complexity of pre-processing imposed by PSM/GPSM is not imposed on SM/GSM.
- the channel knowledge requirement of PSM/GPSM is more demanding than that of SM/GSM, since the former suffers further from potential feedback impairments in addition to the channel estimation errors encountered at the receiver, that are common for both schemes.

In fact, PSM/GPSM may become beneficial in different applications, for example in relay selection. Furthermore, the PSM/GPSM scheme proposed may provide the potential of using efficient power allocation at the transmitter side for the sake of attaining an additional beam-forming gain, which constitutes an important benefit of our PSM/GPSM scheme, as facilitated by the knowledge of the CSIT. More importantly, they may be used in a hybrid manner in conjunction with SM/GSM. Hence, in summary, the PSM/GPSM scheme proposed in this paper constitutes a complement, rather than a competitor of the classic SM/GSM.

III. System Analysis

A. Analytical Average Bit Error Probability

Let us now use the union-bound approach for deriving the analytical Average Bit Error Probability (ABEP) P_e of our GPSM scheme using the joint detection approach, where formally, we have

$$P_e \leq \frac{1}{k_{eff}|\mathcal{B}|} \mathbb{E}\{ \sum_{\boldsymbol{s}_m^k \in \mathcal{B}} \sum_{\boldsymbol{s}_n^j \in \mathcal{B} \neq \boldsymbol{s}_m^k} d(\boldsymbol{s}_m^k, \boldsymbol{s}_n^j) P_r(\boldsymbol{s}_m^k \mapsto \boldsymbol{s}_n^j) \}, \quad (16)$$

where $P_r(\boldsymbol{s}_m^k \mapsto \boldsymbol{s}_n^j)$ denotes the Pairwise Error Probability (PEP) and $d(\boldsymbol{s}_m^k, \boldsymbol{s}_n^j)$ denotes the Hamming distance between the equivalent bit representations of the super-symbol $\boldsymbol{s}_m^k$ and $\boldsymbol{s}_n^j$. Furthermore, the expectation is taken over different channel realizations.

1) ABEP of PSM: The PEP $P_r(\boldsymbol{s}_m^k \mapsto \boldsymbol{s}_n^j)$ of our PSM scheme can be classified according to three different cases [14], namely the errors occurring in the spatial symbol k only, in the conventional modulated symbol b_m only and in both of them jointly. Explicitly, we have

$$P_r(\boldsymbol{s}_m^k \mapsto \boldsymbol{s}_n^j) = \begin{cases} P_K(\boldsymbol{s}_m^k \mapsto \boldsymbol{s}_m^j), & \text{if } m = n, j \neq k \\ P_M(\boldsymbol{s}_m^k \mapsto \boldsymbol{s}_n^k), & \text{if } m \neq n, j = k \\ P_J(\boldsymbol{s}_m^k \mapsto \boldsymbol{s}_n^j), & \text{if } m \neq n, j \neq k. \end{cases} \quad (17)$$

Let us now formulate the expressions for these three cases with the aid of the Q-function.

The PEP $P_K(\boldsymbol{s}_m^k \mapsto \boldsymbol{s}_m^j)$ of *case I* is given by:

$$P_K(\boldsymbol{s}_m^k \mapsto \boldsymbol{s}_m^j) = Q(\beta |b_m| / \sqrt{N_0}). \quad (18)$$

Proof: Let us now consider the first case, where only the spatial symbol is erroneous and hence we have

$$\begin{aligned} P_K(\boldsymbol{s}_m^k \mapsto \boldsymbol{s}_m^j) &= P_r(||\boldsymbol{y}/\beta - \boldsymbol{s}_m^k||^2 > ||\boldsymbol{y}/\beta - \boldsymbol{s}_m^j||^2) \\ &= P_r[|b_m|^2 - 2\mathcal{R}(y_k^* b_m/\beta) > |b_m|^2 - 2\mathcal{R}(y_j^* b_m/\beta)] \\ &= P_r[\mathcal{R}(y_j^* b_m/\beta) - \mathcal{R}(y_k^* b_m/\beta) > 0] \\ &= P_r[\mathcal{R}(b_m^* w_j/\beta) - \mathcal{R}(b_m^* w_k/\beta) > |b_m|^2]. \end{aligned} \tag{19}$$

Since w_j and w_k are independent identical distributed (i.i.d) variables obeying $\mathcal{CN}(0, N_0)$, the Left-Hand-Side (LHS) of (19) is a Gaussian random variable obeying $\mathcal{N}(0, |b_m|^2 N_0/\beta^2)$. As a result, the PEP $P_K(\boldsymbol{s}_m^k \mapsto \boldsymbol{s}_m^j)$ may be written as in (18).

The PEP $P_M(\boldsymbol{s}_m^k \mapsto \boldsymbol{s}_n^k)$ of *case II* is formulated as:

$$P_M(\boldsymbol{s}_m^k \mapsto \boldsymbol{s}_n^k) = Q\left(\beta \frac{(|b_n|^2 + |b_m|^2)/2 - \mathcal{R}(b_m^* b_n)}{|b_n - b_m|\sqrt{N_0/2}}\right). \tag{20}$$

Proof: When considering the second case, where only the conventional modulated symbol is erroneous, we have

$$\begin{aligned} P_M(\boldsymbol{s}_m^k \mapsto \boldsymbol{s}_n^k) &= P_r(||\boldsymbol{y}/\beta - \boldsymbol{s}_m^k||^2 > ||\boldsymbol{y}/\beta - \boldsymbol{s}_n^k||^2) \\ &= P_r[|b_m|^2 - 2\mathcal{R}(y_k^* b_m/\beta) > |b_n|^2 - 2\mathcal{R}(y_k^* b_n/\beta)] \\ &= P_r[\mathcal{R}(y_k^* b_n/\beta) - \mathcal{R}(y_k^* b_m/\beta) > (|b_n|^2 - |b_m|^2)/2] \\ &= P_r[\mathcal{R}(w_k^* b_n/\beta) - \mathcal{R}(w_k^* b_m/\beta) \\ &\quad > \frac{|b_n|^2 + |b_m|^2}{2} - \mathcal{R}(b_m^* b_n)]. \end{aligned} \tag{21}$$

Now the LHS of (21) is a Gaussian random variable obeying $\mathcal{N}(0, |b_n - b_m|^2 N_0/2\beta^2)$. Hence, the PEP $P_M(\boldsymbol{s}_m^k \mapsto \boldsymbol{s}_n^k)$ can be written as in (20).

The PEP $P_J(\boldsymbol{s}_m^k \mapsto \boldsymbol{s}_n^j)$ of *case III* is expressed as:

$$P_J(\boldsymbol{s}_m^k \mapsto \boldsymbol{s}_n^j) = Q\left(\beta \sqrt{\frac{|b_n|^2 + |b_m|^2}{2N_0}}\right). \tag{22}$$

Proof: Finally, when both the spatial symbol and the conventional modulated symbol are erroneous, we have

$$\begin{aligned} P_J(\boldsymbol{s}_m^k \mapsto \boldsymbol{s}_n^j) &= P_r(||\boldsymbol{y}/\beta - \boldsymbol{s}_m^k||^2 > ||\boldsymbol{y}/\beta - \boldsymbol{s}_n^j||^2) \\ &= P_r[|b_m|^2 - 2\mathcal{R}(y_k^* b_m/\beta) > |b_n|^2 - 2\mathcal{R}(y_j^* b_n/\beta)] \\ &= P_r[\mathcal{R}(y_j^* b_n/\beta) - \mathcal{R}(y_k^* b_m/\beta) > (|b_n|^2 - |b_m|^2)/2] \\ &= P_r[\mathcal{R}(b_n^* w_j/\beta) - \mathcal{R}(b_m^* w_k/\beta) > (|b_n|^2 + |b_m|^2)/2]. \end{aligned} \tag{23}$$

Now the LHS of (23) is a Gaussian random variable obeying $\mathcal{N}(0, (|b_n|^2 + |b_m|^2) N_0/2\beta^2)$. Hence, the PEP $P_J(\boldsymbol{s}_m^k \mapsto \boldsymbol{s}_n^j)$ may be written as in (22).

2) ABEP of GPSM: The above analytic formulae provide an insight into the three different error-components of our PSM scheme. When considering the analytical ABEP of GPSM, partitioning the error patterns similar to (17) would be obscure. Instead, we derive it with the aid of the three terms in (19), (21) and (23). The final ABEP of GPSM still follows (16), while the derivation of PEP obeys the following theorem.

Theorem III.1. *The PEP $P_r(\boldsymbol{s}_m^k \mapsto \boldsymbol{s}_n^j)$ of GPSM may be compactly formulated as*

$$P_r(\boldsymbol{s}_m^k \mapsto \boldsymbol{s}_n^j) = Q\left(\beta \frac{B - C}{\sqrt{(D+E)N_0}}\right), \tag{24}$$

where we have

$$B = \sum_{i \in \Psi} \frac{|b_{n_i}|^2 + |b_{m_i}|^2}{2}; \quad C = \sum_{i \in \Psi_1} \mathcal{R}(b_{m_i}^* b_{n_i}); \tag{25}$$

$$D = \sum_{i \in \Psi_0} \frac{|b_{n_i}|^2 + |b_{m_i}|^2}{2}; \quad E = \sum_{i \in \Psi_1} \frac{|b_{n_i} - b_{m_i}|^2}{2}. \tag{26}$$

Proof: Let $\Psi = [k_1, \ldots, k_i, \ldots, k_{N_a}]$ denote the set of activated antenna indices of the activation pattern $\mathcal{C}(k)$, where we have $k_i = \mathcal{C}(k, i)$. Furthermore let $\boldsymbol{z} = \boldsymbol{y}/\beta$ and $\boldsymbol{v} = \boldsymbol{w}/\beta$ for simplification. Then the PEP $P_r(\boldsymbol{s}_m^k \mapsto \boldsymbol{s}_n^j)$ is written as

$$\begin{aligned} P_r(\boldsymbol{s}_m^k \mapsto \boldsymbol{s}_n^j) &= P_r(||\boldsymbol{z} - \boldsymbol{s}_m^k||^2 > ||\boldsymbol{z} - \boldsymbol{s}_n^j||^2) \\ &= P_r[\sum_{i \in \Psi} |b_{m_i}|^2 - 2\mathcal{R}(z_{k_i}^* b_{m_i}) > \sum_{i \in \Psi} |b_{n_i}|^2 - 2\mathcal{R}(z_{j_i}^* b_{n_i})] \\ &= P_r[\sum_{i \in \Psi} \mathcal{R}(z_{j_i}^* b_{n_i}) - \mathcal{R}(v_{k_i}^* b_{m_i}) > \sum_{i \in \Psi} (|b_{n_i}|^2 + |b_{m_i}|^2)/2]. \end{aligned} \tag{27}$$

Furthermore, Ψ_1 denotes the set of activated antenna indices that are correctly detected, i.e. we have $j_i = k_i, \forall i \in \Psi_1$. Similarly, Ψ_0 denotes the complementary set of Ψ_1. Thus (27) is further expanded as in (28). Then it becomes clear that at the LHS of (28), the two summations result in two Gaussian random variables, respectively, obeying

$$\mathcal{N}(0, \sum_{i \in \Psi_0} (|b_{n_i}|^2 + |b_{m_i}|^2) N_0/2\beta^2)$$

$$\mathcal{N}(0, \sum_{i \in \Psi_1} |b_{n_i} - b_{m_i}|^2 N_0/2\beta^2).$$

Hence, the PEP $P_r(\boldsymbol{s}_m^k \mapsto \boldsymbol{s}_n^k)$ may be written as in (24). [1]

B. Robustness Investigations

1) Channel Estimation Error: Like in all transmitter precoding schemes, an important aspect related to GPSM is its resilience to CSIT inaccuracies. When considering a Frequency Division Duplex (FDD) system for example, the cause of this inaccuracy may be many-fold, such as for example the channel estimation errors at the receiver, quantization errors imposed on the CSIT feedback and error-infested imperfect feedback links, which are also outdated. In this paper, we investigate the impact of inaccurate CSIT on our GPSM scheme by assuming that the transmitter is capable of accurately tracking the long term average Channel State Information (CSI), but it is subject to instantaneous CSI errors. This consideration is practical for example in the LTE system, where usually carefully designed periodic pilot patterns are embedded into the payload.

More explicitly, we let $\boldsymbol{H} = \boldsymbol{H}_a + \boldsymbol{H}_i$, where $\boldsymbol{H}_a$ represents the matrix of the average CSI, with each entry obeying the

[1] Note that the PEP derivations of Section III.A were carried out under the perfect CSIT assumption, while more involved numerical integrations are required for the imperfect CSIT scenario for the sake of averaging the effects of CSIT imperfections.

$$P_r[\sum_{i\in\Psi}\mathcal{R}(z_{j_i}^* b_{n_i}) - \mathcal{R}(v_{k_i}^* b_{m_i}) > \sum_{i\in\Psi}(|b_{n_i}|^2 + |b_{m_i}|^2)/2$$
$$= P_r[\underbrace{\sum_{i\in\Psi_0}\mathcal{R}(v_{j_i}^* b_{n_i}) - \mathcal{R}(v_{k_i}^* b_{m_i})}_{\mathcal{N}(0,DN_0/\beta^2)} + \underbrace{\sum_{i\in\Psi_1}\mathcal{R}(v_{k_i}^* b_{n_i}) - \mathcal{R}(v_{k_i}^* b_{m_i})}_{\mathcal{N}(0,EN_0/\beta^2)} > \underbrace{\sum_{i\in\Psi}(|b_{n_i}|^2 + |b_{m_i}|^2)/2}_{B} - \underbrace{\sum_{i\in\Psi_1}\mathcal{R}(b_{m_i}^* b_{n_i})}_{C} \quad (28)$$

complex Gaussian distribution of $h_a \sim \mathcal{CN}(0,\sigma_a^2)$ and $\boldsymbol{H}_i$ is the instantaneous CSI deviation matrix obeying the complex Gaussian distribution of $h_i \sim \mathcal{CN}(0,\sigma_i^2)$, where we have $\sigma_a^2 + \sigma_i^2 = 1$. As a result, only $\boldsymbol{H}_a$ is available at the transmitter, when forming the ZF pre-coder of $\mathbb{P}$. There is a plethora of CSIT inaccuracy counter-measures conceived for general transmitter pre-coding schemes in the literature [28], [29], but they are beyond the scope of our GPSM discussions in this paper.

2) Low-rank Approximation: We now discuss another important aspect associated with GPSM, namely the low-rank pre-coder scenario, while assuming perfect CSIT for the sake of avoiding the potentially obfuscating effects of having multiple combined sources of impairments. Since typical linear pre-coders involve matrix inversion, low-rank pre-coder solutions are preferable, when the matrix dimension is high or when the matrix is ill-conditioned. Originally, the kth column vector $\boldsymbol{p}_k$ of the transmitter pre-coding matrix $\mathbb{P}$ may be written as $\boldsymbol{p}_k = \boldsymbol{R}_D^{-1}\boldsymbol{h}_k^*$, where we have $\boldsymbol{R}_D = \boldsymbol{H}^*\boldsymbol{H}^T$. The low-rank pre-coder design invokes a projection matrix $\mathbb{P}_k \in \mathbb{C}^{N_t\times L}$ for the sake of transforming the original inversion to an L-dimensional subspace of

$$\boldsymbol{p}_k = \boldsymbol{P}_k^*(\boldsymbol{P}_k^T\boldsymbol{R}_D\boldsymbol{P}_k^*)^{-1}\boldsymbol{P}_k^T\boldsymbol{h}_k^*. \quad (29)$$

Typical low-rank pre-coders relying on the first L principal components of the eigen-decomposition of $\mathbb{R}_D$ achieve a low performance [26]. Hence, let us now invoke low-rank pre-coders relying on the Taylor Polynomial (TP) approximation detailed in [26], where $\mathbb{R}_D$ is expanded into its TP representation and the first L terms are then retained to form the projection matrix. According to [26], we have

$$\boldsymbol{P}_k = [\boldsymbol{I}_N, \boldsymbol{R}_D^*, \ldots, \boldsymbol{R}_D^{*L-1}](\boldsymbol{I}_L \otimes \boldsymbol{h}_k), \quad (30)$$

where $\otimes$ stands for the *Kronecker product*.

C. Further Improvements

Let us now conceive further improvements for detecting the proposed GPSM without incurring the performance degradation effects discussed in Section III-B. When separate detection is considered, we can see that (13) is all about determining the correct antenna pattern / spatial symbol by simply sorting the received power accumulated over each receive antenna pattern. The above-mentioned ZF design criterion aims for avoiding any energy leakage to other antenna indices. However, we may be able to improve the above design by allowing energy leakage to the specific antenna indices of the activated antenna pattern. More explicitly, this will naturally improve the detection philosophy of (13), since the quantity $\sum_{i=1}^{N_a}|y_{\mathcal{C}(j,i)}|^2$ will be higher for the intended antenna pattern of $j = k$.

By contrast, this artificial energy leakage will degrade the detection regime of (14), since it introduces ICI upon detecting a particular conventionally modulated symbol. By exploiting the fact that a clear decision boundary exists when detecting a PSK modulated symbol, we can thus shape the ICI in order to minimize its contamination by beneficially aligning its phase with that of the desired signal. In this case, the above-mentioned energy leakage will become beneficial to both the regimes of (13) and of (14).

Mathematically, to construct the beneficially co-phased artificial ICI, we have to rotate the phase of the original ICI relative to the desired signal. Hence, given the super-symbol $\boldsymbol{s}$ and its entry of $s_v = \boldsymbol{\omega}_v\boldsymbol{b}_m, \forall v \in [1, N_r]$, where $\boldsymbol{\omega}_v$ denotes the vth row of $\boldsymbol{\Omega}_k$, the relative phase represented by $\phi_{u,v}$ between s_v and s_u may be shown to become $\phi_{u,v} = \measuredangle s_v - \measuredangle(\rho_{u,v}s_u)$, where $\rho_{u,v}$ is the entry of the Maximal Ratio Transmission (MRT) matrix $\boldsymbol{H}^T\boldsymbol{H}^*$. As a result, the appropriately shaped energy leakage can be constructed by the reinforcement matrix of $\mathbb{R} \in \mathbb{C}^{N_r\times N_r}$, having entries of $r_{u,v} = \phi_{u,v}\rho_{u,v}$. Consequently, our pre-coding matrix of (6) would have to be modified as

$$\boldsymbol{P} = \beta_r\boldsymbol{H}^*(\boldsymbol{H}^T\boldsymbol{H}^*)^{-1}\boldsymbol{R}^T, \quad (31)$$

where we set $\beta_r = \sqrt{N_r/\mathrm{Tr}[\boldsymbol{R}^*(\boldsymbol{H}^T\boldsymbol{H}^*)^{-1}\boldsymbol{R}^T]}$ for ensuring appropriate normalisation, which is typically smaller than the original β.

Let us now see how the reinforcement matrix assists in the detection process of GPSM. Assuming that the vth receive antenna is activated, namely we have $v \in \mathcal{C}(k)$, then the received signal becomes:

$$y_v = \beta_r\rho_{v,v}s_v + \beta_r\sum_{u\in\mathcal{C}(k)/v}\phi_{u,v}\rho_{u,v}s_u + w_v, \quad (32)$$
$$= \beta_r\rho_{v,v}s_v + \beta_r\sum_{u\in\mathcal{C}(k)/v}s_v\frac{\rho_{u,v}^*s_u^*}{|\rho_{u,v}|}\rho_{u,v}s_u + w_v, \quad (33)$$
$$= \beta_r\left(\rho_{v,v} + \sum_{u\in\mathcal{C}(k)/v}|\rho_{u,v}|\right)s_v + w_v. \quad (34)$$

This is in contrast to the conventional GPSM design, where $y_v = \beta s_v + w_v$. Our empirical results provided in the next section will show that the reinforcement matrix arrangement attains a substantially improved BER performance, thanks to the artificial appropriately shaped energy leakage.

IV. Numerical Results

Let us now characterize the Bit Error Ratio (BER) performance of our GPSM scheme in comparison to that of the

TABLE I
EFFECTIVE THROUGHPUT k_{eff} AND DETECTION COMPLEXITY χ OF GPSM AND OF THE CONVENTIONAL MIMO BENCH-MAKER CORRESPONDING TO $N_a = N_r$ (HIGHLIGHTED IN •) FOR DIFFERENT SETTINGS, WHERE $k_{eff} = k_{ssk} + N_a k_{mod}$, $\chi = N_r + M + N_a M$ FOR GPSM, $\chi = M + N_r M$ FOR CONVENTIONAL MIMO.

	N_t	N_r	N_a	M	k_{eff}	χ	
	4/8	2	1	4	3 = 1+1×2	10 = 2+4+1×4	
•	4/8	2	2	4	4 = 0+2×2	12 = 0+4+2×4	
	4/8	2	1	8	4 = 1+1×3	18 = 2+8+1×8	
	8/16	4	1	4	4 = 2+1×2	12 = 4+4+1×4	
	8/16	4	2	4	6 = 2+2×2	16 = 4+4+2×4	
	8/16	4	3	4	8 = 2+3×2	20 = 4+4+3×4	▲
•	8/16	4	4	4	8 = 0+4×2	20 = 0+4+4×4	▲
	8/16	4	1	64	8 = 2+1×6	132 = 4+64+1×64	
	8/16	4	2	8	8 = 2+2×3	28 = 4+8+2×8	
	16	8	1	2	5 = 3+1×2	16 = 8+4+1×4	
	16	8	2	2	8 = 4+2×2	20 = 8+4+2×4	
	16	8	3	2	11 = 5+3×2	24 = 8+4+3×4	
	16	8	4	2	14 = 6+4×2	28 = 8+4+4×4	
	16	8	5	2	15 = 5+5×2	32 = 8+4+5×4	
	16	8	6	2	16 = 4+6×2	36 = 8+4+6×4	■
•	16	8	8	2	16 = 0+8×2	36 = 0+4+8×4	■
	16	8	2	64	16 = 4+2×6	200 = 8+64+2×64	
	16	8	3	16	17 = 5+3×4	72 = 8+16+3×16	

conventional MIMO scheme relying on a full multiplexing capability. We will consider both conventional MIMO settings of $\{N_t, N_r\} = \{[8,2],[8,4]\}$ and the large-dimensional MIMO setting of $\{N_t, N_r\} = \{[16,4],[16,8]\}$. For all different MIMO transmission configurations, we use QPSK only for the data stream's transmissions, except for Fig 2 and Fig 3, where different modulation schemes are employed to match the rate. In Table I, we will list the throughput k_{eff} in terms of the total number of bits conveyed and the complexity χ quantified in terms of the total number of multiplications required at the detector for all different MIMO transmission configurations. In all figures, SNR_b denotes the Signal to Noise Ratio (SNR) per bit.

A. Perfect CSIT

Fig 1 shows the simulated BER performance of both the GPSM scheme and of the conventional MIMO scheme corresponding to $N_a = N_r$, where both the joint and the separate detection as well as the analytical results are portrayed. Both plots show that the analytical results plotted in dashed lines constitute the upper bound of the numerical results. The BER performance of separate detection is represented by the hollow legends, while that of joint detection by the filled legends, which appear to have only marginal performance differences. This is because the ZF pre-coding employed is capable of successfully cancelling the inter-stream interference for the sake of facilitating their separate detection.

In all GPSM configurations investigated in Fig 1 using separate detection, the complexity is no higher than that of the corresponding conventional MIMO benchmark corresponding to $N_a = N_r$, as shown in Table I. Observe that the GPSM scheme achieves a better BER than that of the conventional MIMO scheme corresponding to $N_a = N_r$ in all cases, regardless of their throughput. Naturally, upon increasing the throughput of GPSM by increasing the number of activated antennas, a higher transmit power is required to attain an

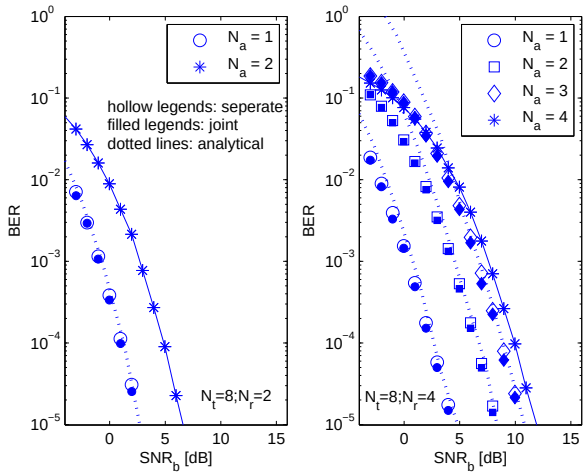

Fig. 1. BER performance of both the GPSM scheme and of the conventional MIMO scheme for both $\{N_t, N_r\} = \{[8,2]\}$ (left plot) and for $\{N_t, N_r\} = \{[8,4]\}$ (right plot).

acceptable BER, as seen in the right plot. For example, to achieve a BER of 10^{-5}, activating $N_a = 2$ requires about 4dB higher power than activating $N_a = 1$.

For $N_a = 3$, the GPSM scheme exhibits an approximately 1dB SNR gain at the BER of $P_e = 10^{-5}$, when compared to the conventional MIMO scheme corresponding to $N_a = N_r$ and this is achieved at the same throughput and complexity, as highlighted by the symbol ▲ in Table I. Note that the difference between these two lies in the specific mapping of the 2 bits of information, which is allocated to the spatial symbol of the GPSM scheme and to the data stream of the conventional MIMO scheme.

B. Rate Match

Fig 2 shows the BER performance of various GPSM configurations created by adjusting the conventional M-ary PSK/QAM throughput of the data streams so as to match the throughput of a full-multiplexing based MIMO scheme using QPSK, where both the associated throughput and the complexity are shown in Table I. Observe in Fig 2 that under the MIMO setting of $\{N_t, N_r\} = \{[8,4]\}$, 64-QAM has to be employed in conjunction with $N_a = 1$ for GPSM for maintaining the desired throughput and hence the resultant BER performance becomes worse than that of the conventional MIMO scheme using QPSK. This is because 64-QAM is a vulnerable scheme, which requires a high SNR. For all other rate-matched scenarios, the GPSM schemes exhibit a significantly better BER performance than the conventional MIMO scheme using QPSK.

Fig 3 shows the rate-match performance of our large-dimensional MIMO. Similar to Fig 2, unless 64-QAM has to be employed for maintaining the desired throughput, which occurs in the cases of $\{N_t, N_r, N_a\} = \{[16,4,1],[16,8,2]\}$, the resultant BER performance of GPSM becomes better than that of the conventional MIMO benck-maker using QPSK. Importantly, the specific GPSM schemes allocating some of their information to conventional M-ary PSK/QAM, such as the $\{N_t, N_r, N_a\} = \{[16,4,2],[16,8,3]\}$ arrangements

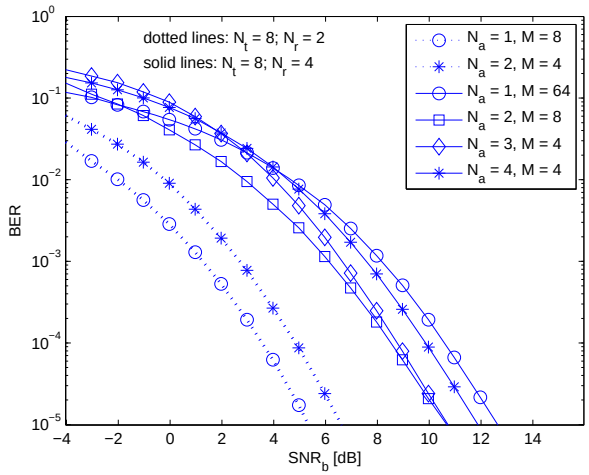

Fig. 2. BER performance of our GPSM scheme in comparison to the identical-rate full multiplexing MIMO bench-mark scheme using QPSK for $\{N_t, N_r\} = \{[8, 2], [8, 4]\}$.

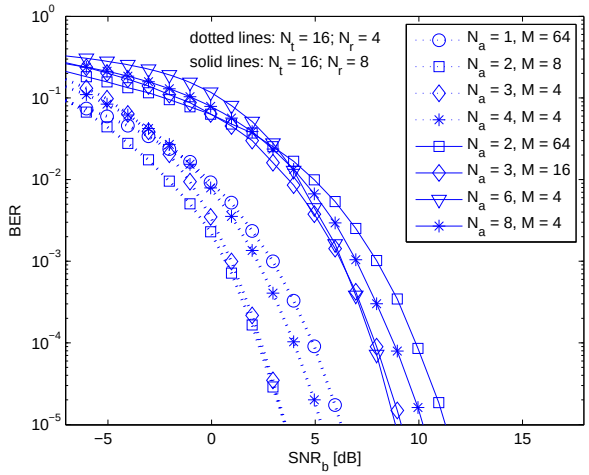

Fig. 3. BER performance of our GPSM scheme in comparison to the identical-rate full multiplexing MIMO bench-mark scheme using QPSK for $\{N_t, N_r\} = \{[16, 4], [16, 8]\}$.

impose a higher detection complexity than those that prefer mapping their information to spatial symbols, namely those corresponding to $\{N_t, N_r, N_a\} = \{[16, 4, 3], [16, 8, 6]\}$. Since the increased complexity only brings about BER performance improvements in the low to medium SNR region, it might be a better design option to allocate information to the spatial symbols right across the entire SNR region, rather than using an SNR-dependent mapping.

C. Imperfect CSIT

Fig 4 and Fig 5 show the BER performance of both the GPSM scheme using separate detection and of the conventional MIMO benchmark scheme, when either a relatively low CSIT error of $\sigma_i = 0.1$ or a severe CSIT error of $\sigma_i = 0.4$ is encountered by the large-dimensional MIMO settings, respectively. Focusing our attention on the perfect CSIT based scenarios shown in dotted lines in both figures, they demonstrate even more explicitly the observations made

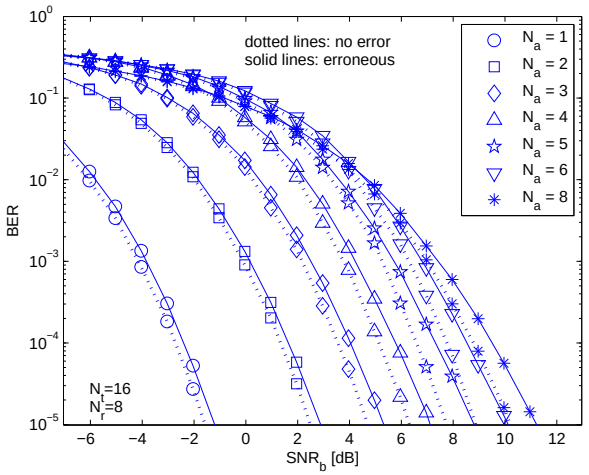

Fig. 4. Impact of CSIT error on the BER performance of both the GPSM scheme and of the conventional MIMO scheme for $\{N_t, N_r\} = \{[16, 8]\}$, where the CSI error was $\sigma_i = 0.1$.

for the standard MIMO settings. Explicitly, the GPSM using $N_a = 6$ achieves in excess of 1dB SNR gain at BER of $P_e = 10^{-5}$, when compared to the conventional MIMO bench-mark scheme having the same throughput and complexity, as highlighted by the symbol ■ in Table I.

When a low CSIT error of $\sigma_i = 0.1$ is considered, Fig 4 shows that the GPSM scheme associated with various configurations is less adversely affected by the CSIT error in comparison to the conventional MIMO bench-mark scheme. As expected, the higher the GPSM throughput, the more grave the BER performance erosion becomes.

When a severe CSIT error of $\sigma_i = 0.4$ is encountered, it can be seen in Fig 5 that a substantially higher BER performance degradation is observed in comparison to that found in Fig 4. When considering various GPSM throughputs having diverse configurations, those supporting a lower throughput exhibit a better resilience against CSIT errors than those supporting a higher throughput, which is in line with our expectations. Although, the BER performance of the GPSM scheme using $N_a = 6$ becomes worse than that of the conventional MIMO scheme for $\sigma_i = 0.4$ because the spatial symbol errors associated with the antenna pattern detection inflict error-precipitation upon the QPSK modem used. However, the BER performance of both schemes remains simply unacceptable for the $\sigma_i = 0.4$ scenarios. Hence, more sophisticated joint iterative channel estimation and data detection methods have to be conceived in conjunction with channel coding.

D. Low-rank Approximation

Fig 6 shows the effect of using TP based low-rank precoders on both the GPSM scheme and on the conventional MIMO bench-mark scheme. As expected, the lower the rank, the worse the performance. Nonetheless, supporting a lower GPSM throughput corresponding to $N_a = 2$, the low-rank approximation remains more robust than in case of a higher GPSM throughput corresponding to $N_a = 3$ and $N_a = 6$.

When considering our GPSM associated with $N_a = 6$ and the conventional bench-mark MIMO, both having the

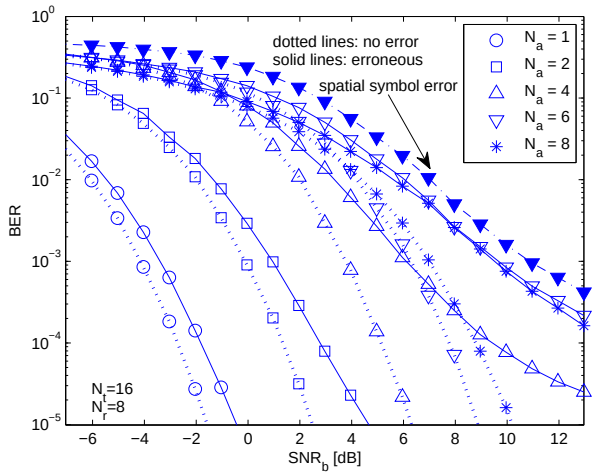

Fig. 5. Impact of CSIT error on the BER performance of both the GPSM scheme and of the conventional MIMO scheme for $\{N_t, N_r\} = \{[16, 8]\}$, where the CSI error was $\sigma_i = 0.4$.

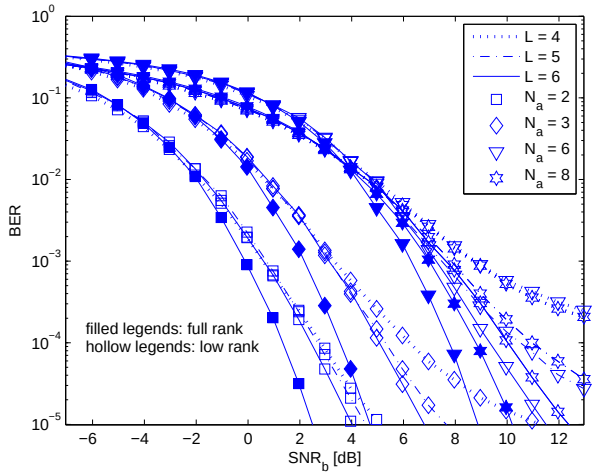

Fig. 6. BER performance of GPSM scheme with TP-based low-rank approximation under $\{N_t, N_r\} = \{[16, 8]\}$.

same throughput, the former maintains a better BER performance for all scenarios having $L > 4$. For $L = 4$, the BER performance of the GPSM scheme using $N_a = 6$ becomes worse than that of the conventional MIMO benchmark scheme, because having an excessively reduced rank results in a degraded antenna pattern detection, which severely affected the BER performance, exhibiting an error floor at $P_e = 10^{-4}$.

E. Reinforcement Matrix-aided GPSM

Fig 7 shows the BER performance of both the conventional and of the reinforcement matrix aided GPSM scheme, where substantial performance improvements are observed across all the simulation scenarios of $N_a = 3, 4, 5, 6$. Quantitatively, to attain the same BER of $P_e = 10^{-5}$, the reinforcement matrix aided GPSM is capable of providing 3-4dB SNR gain, which is due to the beneficial effects of opportunistic energy leakage, as expressed in (34).

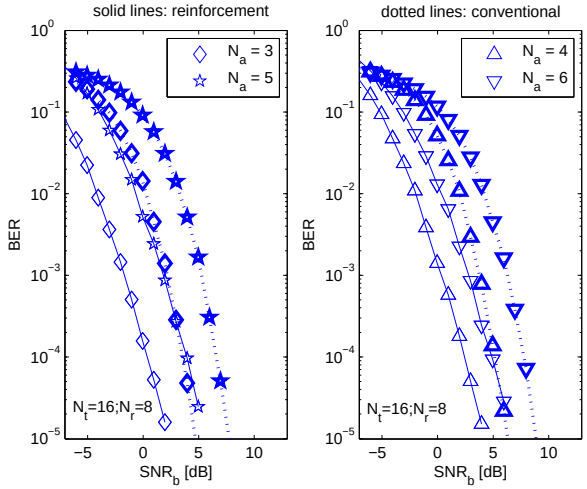

Fig. 7. BER performance of conventional GPSM scheme and reinforcement matrix aided GPSM scheme under $\{N_t, N_r\} = \{[16, 8]\}$.

V. CONCLUSIONS

In this paper, we introduced the concept and design of PSM and its generalisation as a new MIMO transmission scheme. Both numerical and analytical results were provided. Furthermore, the detection complexity of GPSM and its robustness against CSIT error and against a low-rank approximation were also discussed. Our simulation results demonstrated that the GPSM scheme constitutes a promising alternative to the state-of-the-art MIMO arrangements owing to its high flexibility and low complexity in both idealised and realistic environments. Moreover, the benefits of allocating information to the spatial symbols were evidenced in the medium to high SNR region. Importantly, the reinforcement matrix proposed for GPSM attains a further performance improvement.

REFERENCES

[1] L. Hanzo, O. Alamri, M. El-Hajjar, and N. Wu, *Near-Capacity Multi-Functional MIMO Systems: Sphere-Packing, Iterative Detection and Cooperation*, ser. Wiley - IEEE. Wiley, 2009. [Online]. Available: http://books.google.co.uk/books?id=590-JItOJREC

[2] R. Zhang and L. Hanzo, "Wireless cellular networks," *IEEE Veh. Technol. Mag.*, vol. 5, no. 4, pp. 31–39, Dec. 2010.

[3] P. Wolniansky, G. Foschini, G. Golden, and R. Valenzuela, "V-BLAST: An architecture for realizing very high data rates over the rich-scattering wireless channel," in *1998 URSI International Symp. Signals, Syst., Electron.*, Sept.-2 Oct. 1998, pp. 295–300.

[4] S. Alamouti, "A simple transmit diversity technique for wireless communications," *IEEE J. Sel. Areas Commun.*, vol. 16, no. 8, pp. 1451–1458, Oct. 1998.

[5] D. Gesbert, M. Kountouris, R. Heath, C.-B. Chae, and T. Salzer, "Shifting the MIMO paradigm," *IEEE Signal Process. Mag.*, vol. 24, no. 5, pp. 36–46, Sept. 2007.

[6] H. Zhang and H. Dai, "Cochannel channel interference mitigation and cooperative processing in downlink multicell multiuser MIMO networks," *EURASIP J. Wireless Commun. Netw.*, vol. 2004, no. 2, pp. 222–235, Dec. 2004. [Online]. Available: http://dx.doi.org/10.1155/S1687147204406148

[7] T. Marzetta, "Noncooperative cellular wireless with unlimited numbers of base station antennas," *IEEE Trans. Wireless Commun.*, vol. 9, no. 11, pp. 3590–3600, Nov. 2010.

[8] V. R. Cadambe and S. A. Jafar, "Interference alignment and degrees of freedom of the k-user interference channel," *IEEE Trans. Inf. Theory*, vol. 54, no. 8, pp. 3425–3441, Aug. 2008.

[9] A. Mohammadi and F. Ghannouchi, "Single RF front-end MIMO transceivers," *IEEE Commun. Mag.*, vol. 49, no. 12, pp. 104–109, Dec. 2011.

[10] A. Molisch and M. Win, "MIMO systems with antenna selection," *IEEE Microwave Mag.*, vol. 5, no. 1, pp. 46–56, Mar. 2004.
[11] R. Mesleh, H. Haas, S. Sinanovic, C. W. Ahn, and S. Yun, "Spatial modulation," *IEEE Trans. Veh. Technol.*, vol. 57, no. 4, pp. 2228–2241, July 2008.
[12] M. Renzo, H. Haas, and P. Grant, "Spatial modulation for multiple-antenna wireless systems: A survey," *IEEE Commun. Mag.*, vol. 49, no. 12, pp. 182–191, Dec. 2011.
[13] M. D. Renzo, H. Haas, A. Ghrayeb, S. Sugiura, and L. Hanzo, "Spatial modulation for generalized MIMO: Challenges, opportunities and implementation," *Proc. IEEE*. [Online]. Available: http://eprints.soton.ac.uk/354175/
[14] M. Di Renzo and H. Haas, "Bit error probability of SM-MIMO over generalized fading channels," *IEEE Trans. Veh. Technol.*, vol. 61, no. 3, pp. 1124–1144, Mar. 2012.
[15] R. Rajashekar, K. Hari, and L. Hanzo, "Antenna selection in spatial modulation systems," *IEEE Commun. Lett.*, vol. 17, no. 3, pp. 521–524, 2013.
[16] R. Mesleh, M. D. Renzo, H. Haas, and P. M. Grant, "Trellis coded spatial modulation," *IEEE Trans. Wireless Commun.*, vol. 9, no. 7, pp. 2349–2361, July 2010.
[17] E. Basar, U. Aygolu, E. Panayirci, and H. Poor, "Space-time block coded spatial modulation," *IEEE Trans. Commun.*, vol. 59, no. 3, pp. 823–832, Mar. 2011.
[18] J. Jeganathan, A. Ghrayeb, L. Szczecinski, and A. Ceron, "Space shift keying modulation for MIMO channels," *IEEE Trans. Wireless Commun.*, vol. 8, no. 7, pp. 3692–3703, July 2009.
[19] S. Sugiura, S. Chen, and L. Hanzo, "Generalized space-time shift keying designed for flexible diversity-, multiplexing- and complexity-tradeoffs," *IEEE Trans. Wireless Commun.*, vol. 10, no. 4, pp. 1144–1153, Apr. 2011.
[20] A. Younis, N. Serafimovski, R. Mesleh, and H. Haas, "Generalised spatial modulation," in *2010 Conf. Record Forty Fourth Asilomar Conf. Signals, Syst., Comput. (ASILOMAR)*, Nov. 2010, pp. 1498–1502.
[21] J. Wang, S. Jia, and J. Song, "Generalised spatial modulation system with multiple active transmit antennas and low complexity detection scheme," *IEEE Trans. Wireless Commun.*, vol. 11, no. 4, pp. 1605–1615, Apr. 2012.
[22] L.-L. Yang, "Transmitter preprocessing aided spatial modulation for multiple-input multiple-output systems," in *IEEE 73rd Veh. Technol. Conf. (VTC Spring)*, May 2011, pp. 1–5.
[23] A. Stavridis, S. Sinanovic, M. D. Renzo, and H. Haas, "Transmit precoding for receive spatial modulation using imperfect channel knowledge," in *IEEE 75th Veh. Technol. Conf. (VTC Spring)*, May 2012, pp. 1–5.
[24] S. Sugiura, S. Chen, and L. Hanzo, "A universal space-time architecture for multiple-antenna aided systems," *IEEE Commun. Surveys Tuts.*, vol. 14, pp. 401–420, Second Quarter 2012.
[25] A. Goldsmith, *Wireless Communications*. Cambridge University Press, 2005.
[26] L.-L. Yang, "Capacity and error performance of reduced-rank transmitter multiuser preprocessing based on minimum power distortionless response," *IEEE Trans. Wireless Commun.*, vol. 7, no. 11, pp. 4646–4655, Nov. 2008.
[27] Q. Spencer, A. Swindlehurst, and M. Haardt, "Zero-forcing methods for downlink spatial multiplexing in multiuser MIMO channels," *IEEE Trans. Signal Process.*, vol. 52, no. 2, pp. 461–471, Feb. 2004.
[28] D. Gesbert, "Robust linear MIMO receivers: A minimum error-rate approach," *IEEE Trans. Signal Process.*, vol. 51, pp. 2863–2871, Nov. 2003.
[29] X. Zhang, D. Palomar, and B. Ottersten, "Statistically robust design of linear MIMO transceivers," *IEEE Trans. Signal Process.*, vol. 56, pp. 3678–3689, Aug. 2008.

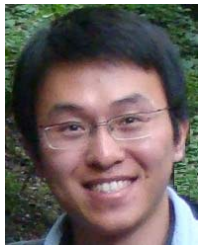

Rong Zhang (M'09) received his PhD (Jun 09) from Southampton University, UK and his BSc (Jun 03) from Southeast University, China. Before doctorate, he was an engineer (Aug 03-July 04) at China Telecom and a research assistant (Jan 06-May 09) at Mobile Virtual Center of Excellence (MVCE), UK. After being a post-doctoral researcher (Aug 09-July 12) at Southampton University, he took industrial consulting leave (Aug 12-Jan 13) for Huawei Sweden R& D as a system algorithms specialist. Since Feb 13, he has been appointed as a lecturer at CSPC group of ECS, Southampton University. He has 25+ journals in prestigious publication avenues (e.g. IEEE, OSA) and many more in major conference proceedings. He regularly serves as reviewer for IEEE transactions/journals and has been several times as TPC member/invited session chair of major conferences. He is the recipient of joint funding of MVCE and EPSRC and is also a visiting researcher of Nanjing University under Worldwide University Network (WUN). More details can be found at http://www.ecs.soton.ac.uk/people/rz

Lie-Liang Yang (M'98, SM'02) received his BEng degree in communications engineering from Shanghai TieDao University, Shanghai, China in 1988, and his MEng and PhD degrees in communications and electronics from Northern (Beijing) Jiaotong University, Beijing, China in 1991 and 1997, respectively. From June 1997 to December 1997 he was a visiting scientist of the Institute of Radio Engineering and Electronics, Academy of Sciences of the Czech Republic. Since December 1997, he has been with the University of Southampton, United Kingdom, where he is the professor of wireless communications in the School of Electronics and Computer Science. Dr. Yang's research has covered a wide range of topics in wireless communications, networking and signal processing. He has published over 290 research papers in journals and conference proceedings, authored/co-authored three books and also published several book chapters. The details about his publications can be found at http://www-mobile.ecs.soton.ac.uk/lly/. He is a fellow of the IET, served as an associate editor to the *IEEE Trans. on Vehicular Technology* and *Journal of Communications and Networks* (JCN), and is currently an associate editor to the *IEEE Access* and the *Security and Communication Networks (SCN) Journal*.

Lajos Hanzo (FREng, FIEEE, FIET, Fellow of EURASIP, DSc) received his degree in electronics in 1976 and his doctorate in 1983. In 2009 he was awarded the honorary doctorate "Doctor Honoris Causa" by the Technical University of Budapest. During his 37-year career in telecommunications he has held various research and academic posts in Hungary, Germany and the UK. Since 1986 he has been with the School of Electronics and Computer Science, University of Southampton, UK, where he holds the chair in telecommunications. He has successfully supervised 80+ PhD students, co-authored 20 John Wiley/IEEE Press books on mobile radio communications totalling in excess of 10 000 pages, published 1300+ research entries at IEEE Xplore, acted both as TPC and General Chair of IEEE conferences, presented keynote lectures and has been awarded a number of distinctions. Currently he is directing a 100-strong academic research team, working on a range of research projects in the field of wireless multimedia communications sponsored by industry, the Engineering and Physical Sciences Research Council (EPSRC) UK, the European Research Council's Advanced Fellow Grant and the Royal Society's Wolfson Research Merit Award. He is an enthusiastic supporter of industrial and academic liaison and he offers a range of industrial courses. He is also a Governor of the IEEE VTS. During 2008 - 2012 he was the Editor-in-Chief of the IEEE Press and a Chaired Professor also at Tsinghua University, Beijing. His research is funded by the European Research Council's Senior Research Fellow Grant. For further information on research in progress and associated publications please refer to http://www-mobile.ecs.soton.ac.uk. Lajos has 17 000+ citations.